Exploring the Structure–Solubility Relationship of Asphaltene Models in Toluene, Heptane, and Amphiphiles Using a Molecular Dynamic Atomistic Methodology

ARTICLE *in* THE JOURNAL OF PHYSICAL CHEMISTRY A · SEPTEMBER 2011

Impact Factor: 2.69 · DOI: 10.1021/jp204319n · Source: PubMed

5 AUTHORS, INCLUDING:

Yosslen Aray
Venezuelan Institute for Scientific Research
66 PUBLICATIONS **728** CITATIONS
SEE PROFILE

José G. Parra
Universidad de Carabobo, UC
8 PUBLICATIONS **11** CITATIONS
SEE PROFILE

David Santiago Coll
Venezuelan Institute for Scientific Research
33 PUBLICATIONS **253** CITATIONS
SEE PROFILE

THE JOURNAL OF PHYSICAL CHEMISTRY A

ARTICLE

pubs.acs.org/JPCA

Exploring the Structure−Solubility Relationship of Asphaltene Models in Toluene, Heptane, and Amphiphiles Using a Molecular Dynamic Atomistic Methodology

Yosslen Aray,*[,†] Raiza Hernández-Bravo,[†] José G. Parra,[‡] Jesús Rodríguez,[†] and David S. Coll[†]

[†]Centro de Química, Instituto Venezolano de Investigaciones Científicas, IVIC, Apartado 21827, Caracas 1020 A, Venezuela

[‡]Facultad Experimental de Ciencias y Tecnología, Departamento de Química, Laboratorio Química Computacional, Universidad de Carabobo, Carabobo, Venezuela

ABSTRACT: The solubility parameters, δ, of several asphaltene models were calculated by mean of an atomistic *NPT* ensemble. Continental and archipelago models were explored. A relationship between the solubility parameter and the molecule structure was determined. In general, increase of the fused-rings number forming the aromatic core and the numbers of heteroatoms such as oxygen, nitrogen, and sulfur produces an increase of the solubility parameter, while increases of the numbers and length of the aliphatic chains yield a systematic decrease of this parameter. Molecules with large total carbon atom number at the tails, n_c, and small aromatic ring number, n_r, exhibit the biggest values of δ, while molecules with small n_c and large n_r show the smallest δ values. A good polynomial correlation $\delta = 5.967(n_r/n_c) - 3.062(n_r/n_c)^2 + 0.507(n_r/n_c)^3 + 16.593$ with $R^2 = 0.965$ was found. The solubilities of the asphaltene models in toluene, heptane, and amphiphiles were studied using the Scatchard−Hildebrand and the Hansen sphere methodologies. Generally, there is a large affinity between the archipelago model and amphiphiles containing large aliphatic tails and no aromatic rings, while continental models show high affinity for amphiphiles containing an aromatic ring and small aliphatic chains.

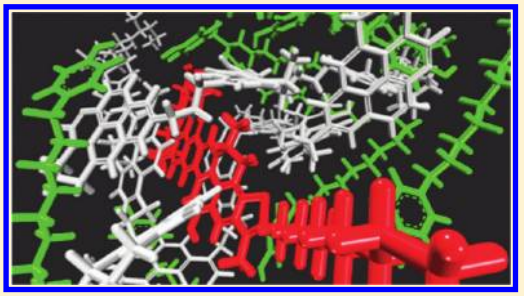

1. INTRODUCTION

Asphaltenes are the heaviest and most complex fraction of crude oil.[1] This fraction plays a major role in the formation of deposits that affect the worldwide crude oil production,[2] and they are commonly presumed to represent the most refractory and difficult portion of the feedstock to process. Asphaltenes are the most aromatic and highest molecular weight portion of crude oil and are defined as the fraction that is soluble in toluene or benzene and insoluble in low-boiling alkanes such as *n*-pentane or *n*-heptane.[2] Asphaltenes are the most viscous and most polar crude oil components; maltenes are the least viscous and most nonpolar components; and resins are between both components.

"If you want to understand function, study structure" advises Francis Crick.[3] Without structural information, predictive science is generally precluded and phenomenology prevails.[4] The functional issues (such as the structure−solubility relationship) of asphaltenes are of enormous importance in the production, transportation, and refining of crude oil.[4] Experimental investigation of the microstructure of heavy crude oil is proven to be difficult because of the strong dependency on the experimental conditions and also the absence of effective approaches.[5−7] Molecular simulation is one way to predict the macroscopic properties that result from specified microscopic molecular interaction and structures.[8] Several average molecular structures for asphaltenes and resins have been recommended.[4,8−16] Two molecular structures emerge from those studies: the continental model is shaped "like your hand", with an aromatic core (palm) with associated alicyclic rings, and with alkyl groups hanging off the periphery (fingers), while the archipelago model consists of smaller aromatic groups linked by aliphatic bridges.

On the other hand, the solubility parameter, δ, is related to the square root of the cohesive energy density, the amount of energy needed to completely remove a unit volume of molecules from their neighbors to an infinite separation. It measures the strength of interactions between molecules in the condensed phase.[17,18] A huge amount of work[18] along the years has demonstrated the versatility of δ to deal with solubility and other properties of petroleum and fossil solids and liquids providing good grounds for application to related issues such as affinity between asphaltene fractions and affinity for solvents and other compounds with a given δ.[18] In the present paper the solubility parameters for a series of reported asphaltenes and amphiphiles using the molecular dynamic methodology were determined. The molecular structure−δ relationship was explored using the molecular connectivity indices of Hall and Kier[19] and a genetic function approximation (GFA)[20] methodology. The solubility of those models in toluene, *n*-heptane, and a set of amphiphiles was studied using the Scatchard−Hildebrand theory for regular liquids and the Hansen sphere methodology.[17]

Received: May 9, 2011
Revised: September 8, 2011
Published: September 09, 2011

2. THEORY FRAMEWORK

2. 1. Solubility Models. The calculated δ makes it possible to explore the solubility of the asphaltenes in solvent such as toluene and *n*-heptane using the Scatchard−Hildebrand[17] theory, in which, the relative solubility, ΔS_R, is calculated using the following:

$$\Delta S_R = \exp\left[-\frac{V_{asphal}}{RT}(\delta_{solv} - \delta_{asphal})^2\right] \quad (1)$$

where V_{asphal}, δ_{solv}, and δ_{asphal} are the asphaltene molar volume and the solubility parameters of the solvent and asphaltene, respectively. In this theory, the maximum of solubility is observed when the asphaltene and solvent cohesive energy density are identical ($\delta_{solv} = \delta_{asphal}$ and $\Delta S_R = 1$). In principle, this simple method allows a satisfactory solubility prediction with a large range of solutes in nonpolar solvents. However, inconsistencies such as that good and bad solvent[18] could have the same δ values have been reported. The sphere method developed by Hansen[17] is an alternative procedure and has been reported as an appropriated methodology to explore the asphaltene solubility.[18] According to Hansen,[17] the solubility of asphaltenes (such as a polymer) in organic liquids is described in the coordinates of the solubility parameter components by a spherical solubility region centered at the asphaltene. The boundaries of the solubility region are given by the radius *R*:

$$R = \sqrt{4(\delta_d^{asphal} - \delta_d^{solvent})^2 + (\delta_p^{asphal} - \delta_p^{solvent})^2 + (\delta_H^{asphal} - \delta_H^{solvent})^2} \quad (2)$$

where δ_d, δ_p, and δ_H are the dispersive, electrostatic, and hydrogen-bond components of δ. A measure for the solubility in a defined solvent is the RED number, defined as the distance RA of the solubility parameter of solvent from the center of the sphere divided by the radius of the sphere R_0:

$$RED = \frac{RA}{R_0} \quad (3)$$

RA is calculated similarly to eq 2. For good (bad) solvents RED ≤ 1 (RED ≥ 1). RED values were found[18] consistent with all known solubility properties of asphaltenes: soluble in aromatic hydrocarbon solvents such as benzene, toluene, ethyl benzene, cumene, and 1-methylnaphthalene (1MN) and also low RED values (high solubility) for *o*-dichlorobenzene, nitrobenzene, quinoline, and pyridine were correctly found. The method also gives RED > 1 for both aliphatic and alicyclic solvents such as *n*-hexane, *n*-pentane, *n*-octane, cyclopentane, and decaline, etc.[18] Additionally, a good linear correlation between RED values and the *n*-heptane volume, V_h, of flocculation experiments corresponding to samples of asphaltene−1MN was also established.[18] The determination of flocculation points of crude oil or crude oil products is one of the practicable methods to range the stability of crude oil products.[21]

2. 2. Molecular Connectivity. Molecular connectivity is a method of molecular structure quantitation[19,20a] in which weighted counts of substructure fragments are incorporated into numerical indices (descriptors). Structural features such as size, branching, unsaturation, heteroatom content, and cyclicity are encoded. Molecular descriptors are calculated, and a mathematical regression linking the property of interest and the descriptors is generated. Topological indices developed by Kier and Hall[19] are a way to encode size, degree of branching, flexibility,

Table 1. Calculated Solubility Parameters ($MPa^{0.5}$) and Electrostatic and Dispersive Components for Benzene, Naphthalene, and Polyaromatic Moities, Estimated from *NPT* Molecular Dynamic Simulations[a]

	reported			this work		
molecule	δ	δ_{vdW} [b]	δ_{elec} [b]	δ	δ_{vdW}	δ_{elec}
benzene	18.8 [b]	18.4	2.0	18.807	18.087	5.134
naphthalene	20.3 [b]	19.2	6.23	20.309	19.613	5.353
A10	24.5 [c]			23.842	23.623	3.154
A11	25.2 [c]			24.405	24.269	2.525
A12	26.1 [c]			25.117	25.227	1.063
n-heptane	15.3 [b]	15.3	0.000	15.314	15.298	0.698
toluene	18.2 [b]	18.0	1.4	18.595	17.931	4.921

[a] Heptane and toluene solvents have been included. [b] Experimental.[25f] [c] Predicted by molecular descriptors.[25e]

and the overall shape of molecules into connectivity indices, χ, a bond additive mathematical invariant of molecules. These indices are two-dimensional (2D) descriptors based on graph theory concepts. The indices calculations start with the reduction of the molecule to the hydrogen-suppressed skeleton or graph. The atoms and bonds assign the vertex and edges of the graph. Each vertex is assigned two atom descriptors based upon the count of σ electrons or valence electrons present,

$$\varsigma = \sigma - h \quad (4)$$

$$\varsigma^v = \frac{\sigma + \pi + n - h}{Z - Z^v - 1} \quad (5)$$

where σ, h, π, n, Z, and Z^v are the number of electrons in σ bonds to all neighbors, the number of hydrogen atoms bonded to an atom, the number of π electrons, the number of lone pairs, the atomic number, and the number of valence electrons in the atom, respectively.

Subgraphs for a molecular graph[19,20a] are defined by the decomposition of the skeleton into fragments of single atoms (zero-order, $m = 0$), a single-edge or one-bond paths (first-order, $m = 1$), two connected edges or two-bond paths (second-order, $m = 2$), three contiguous edges in which no vertex is included twice (third-order path, $m = 3$, $t = P$), clusters (three atoms attached to a central atom, $m = 3$, $t = C$), and so forth. Connectivity χ indices are defined as follows:

$${}^m\chi_t = \sum_k \prod_i (\varsigma_i)_k^{-1/2} \quad (6)$$

k sum over all type t subgraphs with m edges and i over all the vertices (atoms).

In general, ${}^0\chi$ only encode molecule size and ${}^1\chi$ and ${}^2\chi$ encode molecule size and skeletal degree of branching. These indices give little information about the organization of branching within the skeleton. An important graph feature encoded in ${}^3\chi_p$ is the adjacency of branch points. The path-3 index is larger for an adjacent branch point than for separated branch points.

The molecular flexibility index,[19] φ, is a descriptor based on the structural properties that prevent a molecule from being infinitely flexible, i.e., the model for which is an endless chain of $C(sp^3)$ atoms. The structural features considered to prevent a molecule from attaining infinite flexibility mainly are fewer atoms, the presence of rings, and branching. φ encodes these

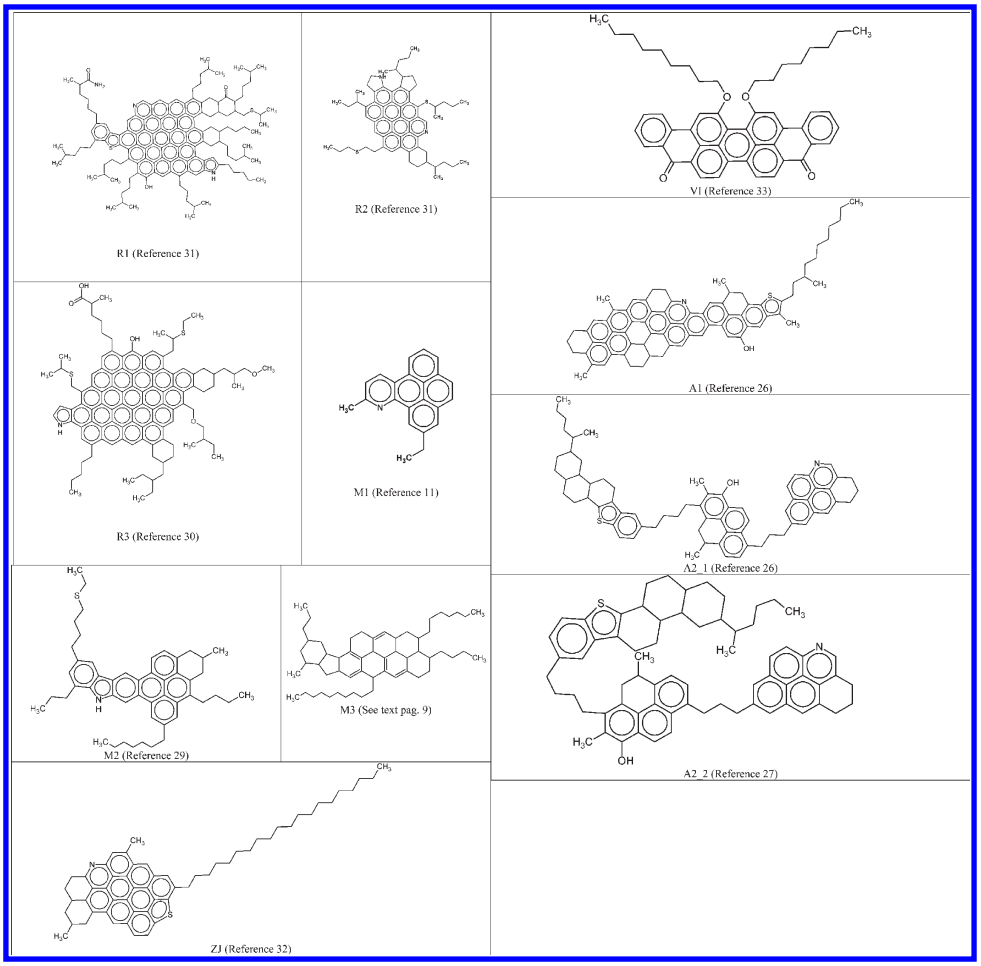

Figure 1. Structures of the asphaltene molecules used in this work. R1 and R2: Reproduced with permission from ref 31. Copyright 1995 Elsevier. R3: Reproduced with permission from ref 30. Copyright 2002 Taylor and Francis. M1: Reprinted with permission from ref 11. Copyright 2000 American Chemical Society. M2: Reprinted with permission from ref 29. Copyright 2001 Taylor and Francis. ZJ: Reprinted with permission from ref 32. Copyright 1994 Scanning Microscopy International. VI: Reprinted with permission from ref 33. Copyright 2009 American Chemical Society. A1 and A2_1: Reprinted with permission from ref 26. Copyright 2005 American Chemical Society. A2_2: Reprinted with permission from ref 27. Copyright 2007 American Chemical Society.

features in the following definition,

$$\varphi = \frac{1k^{\alpha}2k^{\alpha}}{N} \tag{7}$$

where $1k^{\alpha}$ and $2k^{\alpha}$ are the Kier α-modified shape indices[19,20a] and N is the number of vertices (atoms) of the graph.

3. METHODOLOGY OF CALCULATIONS

Molar volume, density, and solubility parameter of model asphaltenes and resins can be calculated by running molecular dynamics at constant pressure and temperature for a cell under periodic boundary conditions, i.e., *NPT* simulations.[22] In this work, Discover software with Compass force field[23] for the *NPT* simulations was used. The atomic charges for the electrostatic component of the force field were determined from quantum mechanical calculations on isolated molecule models with the Dmol3 program[24] by fitting the molecular electrostatic potential, ESP. Amorphous Builder was used to create an initial random and low-density sample using a suitable Monte Carlo procedure to achieve a right distribution of conformational states. In general, we have used the following methodology:

(1) A cubic periodic unit cell containing 10−50 molecules (1000−2000 atoms) for asphaltenes and resins, respectively, at a low density (typically = 0.5−0.65) is built using Amorphous Builder.

(2) The potential energy of the cell is minimized for 5000 steps or until the atom rms force converges to 0.10 kcal/(mol·Å).

(3) Annealing using canonical fixed volume dynamics (*NVT*) ensures appropriate configurations where the molecules can freely interact, typically 750−5000 steps (1 fs/step) at a high temperature of usually 700 K.

(4) *NPT* of 100 000 steps at 300 K thermalizes and equilibrates the system.

(5) *NPT* is restarted for 100 000 additional steps to measure the properties. Molar volume, density, and cohesion energy are calculated along the trajectory, finally averaging the calculated values. The cohesion energies are calculated by subtracting the potential energy of the bulk system from the sum of the potential energies of the individual molecules in vacuum.

(6) This process is repeated N times, with different initial random conformations and packing. N = 10 could be adequate.

Table 2. Asphaltenes Density (ρ), H/C Ratio, Molar Volume (V_m), Solubility Parameter and the Corresponding Electrostatic and Dispersive Components, δ, δ_{elec}, δ_{vdW}, Estimated from *NPT* Molecular Dynamic Simulations

models	ρ (g/cm^3)	H/C	V_m (cm^3/mol)	δ (MPa$^{1/2}$)	δ_{elec} (MPa$^{1/2}$)	δ_{vdW} (MPa$^{1/2}$)
M3	0.965	1.554	802.363	16.889	1.382	16.832
R1	1.065	1.136	1874.035	16.997	4.404	16.416
A2_2	1.096	1.087	881.401	17.722	3.761	17.318
R2	1.102	1.169	860.933	18.292	2.280	18.149
A2_1	1.089	1.087	884.673	18.593	4.965	17.918
		1.020		19.935 [a]	3.640 [a]	19.60 [a]
M2	1.038	1.220	682.126	18.705	3.608	18.353
R3	1.167	0.973	1359.292	19.182	4.358	18.680
ZJ	1.108	1.105	720.058	19.480	0.655	19.469
VI	1.142	0.738	624.330	19.908	4.733	19.337
A1	1.179	0.893	873.347	20.045	3.412	19.752
		0.920		21.3 [a]	4.405 [a]	20.90 [a]
RH1	1.191	0.847	877.059	20.152	3.445	19.855
RH2	1.274	0.683	748.226	20.872	3.772	20.528
M1	1.152	0.773	256.433	21.353	3.476	21.068
RH3	1.299	0.556	696.197	27.415	18.382	20.339
RH4	1.328	0.492	636.735	30.299	22.284	20.529

[a] Reference 18.

The generic COMPASS force field has been extensively optimized to reproduce heats of vaporization of a large number of organic liquids.[22a] Sun[25a] has calculated heats of vaporization for 100 compounds to within an average percent error of experiment of 0.2%. For benzene and alkyl benzene, such as toluene and isoxylene, this force field yields good agreement with the experiment data. COMPASS was employed[25b] to compute solubility parameters for Ultem, a phenyl oligomer; related molecules; and solvent molecules including toluene. The calculated solubility parameter for toluene was 0.07 (cal/cm^3)$^{1/2}$ closer to the average experimental value (8.94 (cal/cm^3)$^{1/2}$) than the previous PCFF force field value.[25c] Recently,[25d] the solubility parameter of indomethacin, a molecule containing two conjugation rings and several heteroatoms, was reported using COMPASS. A good agreement (23.9 MPa$^{0.5}$) with the value computed using the group methods of Van Kravelen (23.3) and Hoy (21.9) was found. Group contribution methods are based on the knowledge of structural fragments within the molecules. Such theoretical models are typically applicable for simple molecular structures, wherein van der Waals forces predominate and have limitations when dealing with complex molecules containing highly directional interactions (hydrogen bonding) or long-range interactions (e.g., electrostatic).[25d]

For extended conjugation systems and fused rings, such as biphenyl and naphthalene, the current functional form of COMPASS was suggested[25a] to be not flexible enough, because the electrons are partially localized in a certain region so that all C−C bonds are not equivalent. The only information to define a bond in that force field is the atom types of the two atoms that are bonded together. Thus, all C−C bonds in and between the aromatic ring forming the asphaltene core are treated using the same atom type of *c3a*. To check this matter, the current authors have calculated the solubility parameter for benzene, naphthalene, and three polyaromatic moieties recently reported[25e] that contain a core of 10, 11, and 12 fused aromatic rings. The parameters for these moieties were determined using correlations with molecular descriptors. The experimental values for benzene and naphthalene[25f] and the reported values for A10, A11, and A12 are listed along with our calculated solubility parameter values in Table 1. Additionally the values for heptane and toluene, the solvents considered in the present studied, were also included in Table 1. A good agreement for benzene and naphthalene can be observed, while our predicted values for the polyaromatic moieties are around 5% smaller than those determined using molecular descriptors. However, note that the trend is exactly reproduced by COMPASS. In fact, a linear relationship $\delta_{reported} = 0.8567\delta_{calcd} + 2.8153$ with $R^2 = 0.999$ was found. Additionally, in Table 1 are collected the contribution of the dispersive and electrostatic component to the total δ value.

Experimental values often list three components for δ: van der Waals (dispersive), Coulombic, and H-bonding. Due to the last two may be considered as electrostatic components, most generic force fields do not contain a separate term for H-bonding, calculations given a van der Waals, δ_{vdW} and an electrostatic, δ_{ES}, component, where $\delta_{ES} = (\delta_C + \delta_H)^{0.5}$, δ_C and δ_H being the Coulombic and H-bonding components of the solubility parameter, respectively. It can be observed from Table 1 that the dispersive components are reproduced well with these simulations, while the biggest deviation was obtained for the electrostatic component of benzene. A similar result using COMPASS has been reported even for ionic liquids.[25g] Note that for these kinds of fused ring compounds, δ_{vdW} completely dominates the solubility parameter values and consequently the general trends of δ is correctly reproduced.

4. RESULTS AND DISCUSSION

4. 1. Asphaltenes Solubility Parameters. Several proposed molecular structures of asphaltenes were chosen from literature reports,[26−33] and they are shown in Figure 1. Nine continental molecular models of asphaltenes containing from 5 to 23 fused aromatic rings at the core, heteroatoms (N, O, S) and 1−11 side aliphatic chains of different length were studied. Two configurations (A2_1 and A2_2) of an archipelago model with three small

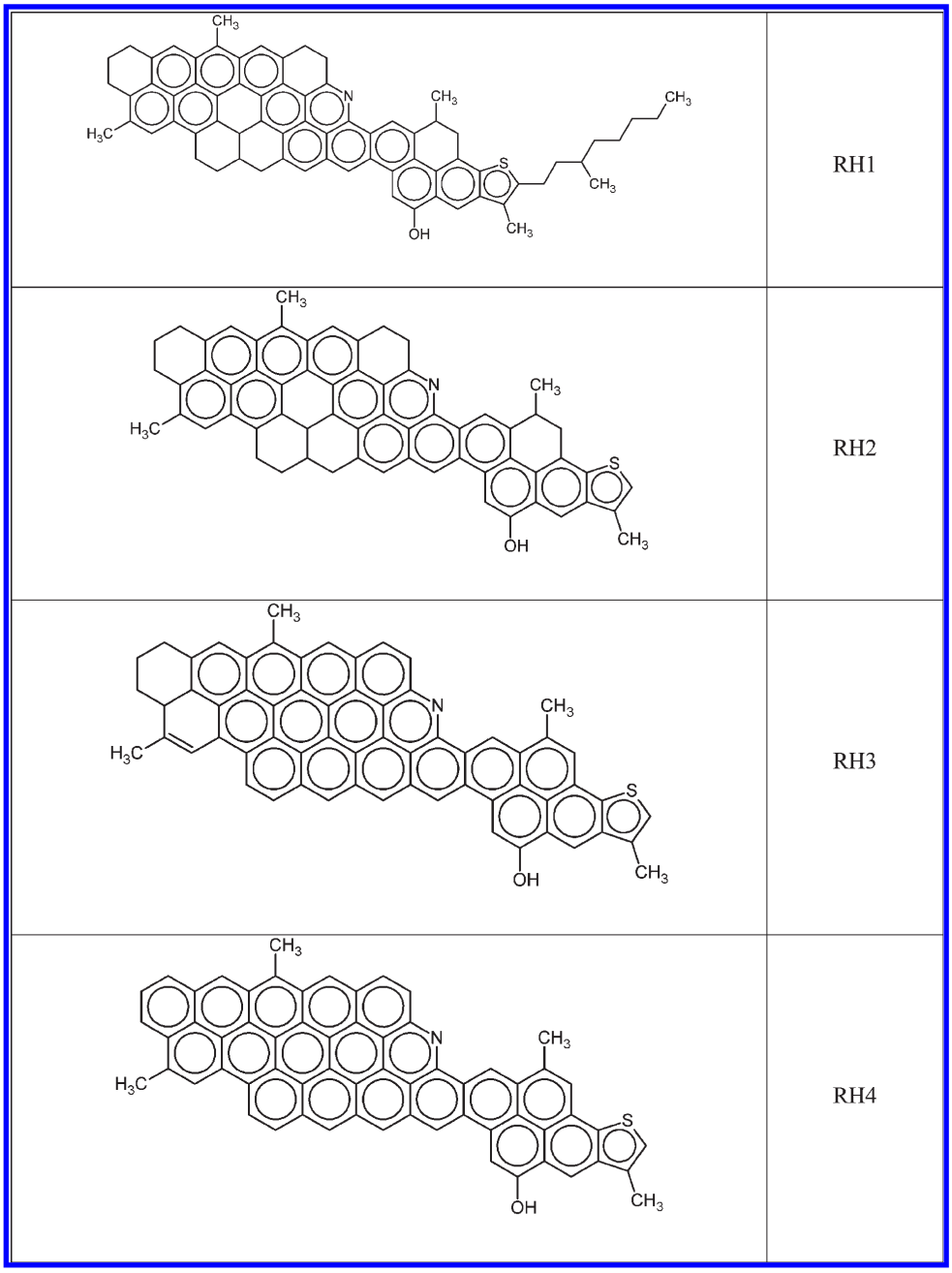

Figure 2. Asphaltene models obtained from A1 Socrates model, removing and increasing the aliphatic tails and aromatic ring numbers, respectively.

aromatic islands were also included. Additionally, to highlight the aromatic rings role, a model (M3) based in the M2 asphaltenes in which all the aromatic rings were removed was included. The density (g/cm^3), *H*/*C* ratio, molar volume (cm^3/mol), solubility parameters (MPa$^{0.5}$), and the corresponding electrostatic and dispersive components resulting from the *NPT* simulations are collected in Table 2. Significant differences (<4.47 MPa$^{0.5}$ in a range of 16.89−21.36 values) among the studied models can be observed. The biggest difference corresponds to the M3 and M1 Mullins models. M1 contains five fused aromatic rings and two small aliphatic chains while M3 does not contain aromatic rings and has five aliphatic tails: one *n*-C_{10}, one *n*-C_7, and three small tails. A variation of 2.564 between the R1 and R3 models was obtained. Both models contain an aromatic core with 23 rings. However, 11 *n*-C_6 and seven *n*-C_5 tails are contained by R1 and R3 models, respectively. Similarly, a difference of 2.32 MPa$^{0.5}$ was determined between the A1 and A2_2 Socrates models. A1 is a continental asphaltene whose core possesses 14 aromatic rings and five aliphatic tails, one -C_{12} and four -C_1, while A2_2 is an archipelago type asphaltene with three aromatic islands with four, three, and two aromatic rings with one *n*-C_6 and two -C_1 tails. We can see in the above cases a behavior that is apparently general for molecules such as asphaltenes: the increase of the core aromatic ring number and decrease of the aliphatic tails number produces an increasing on δ. To go deeply in this asphaltenes behavior, we have systematically removed aliphatic chains and increased the aromatic ring numbers to the Socrates A1 model, creating the RH1, RH2, RH3, and RH4 models (see Figure 2). The calculated

Table 3. Structural Characteristics of the Studied Asphaltene Molecules[a]

model	n_t [b]	n_c [c]	n_{tr} [d]	n_r [e]	total heteroatom no.	n_r/n_c
M3	5	25	7	0	1	0
R1	11	66	26	23	6	0.348
A2_2	3	8	14	4	3	1.125
				3		
				2		
R2	5	25	13	10	3	0.400
A2_1	2	8	14	4	3	1.125
				3		
				2		
tolueno	1	1		1	0	
M2	5	22	8	7	1	0.318
R3	7	35	25	23	6	0.657
ZJ	1	20	12	12	1	0.600
VI	2	16	9	9	4	0.563
A1	5	16	19	13	3	0.813
RH1	5	13	19	13	3	1.000
RH2	4	4	19	13	3	3.250
M1	2	3	5	5	1	1.667
RH3	4	4	19	18	3	4.500
RH4	4	4	19	19	3	4.750

[a] The aromatic rings for the three islands of the archipelago models (see Figure 1) are separately counted. [b] n_t = aliphatic tails number. [c] n_c = total carbon number at the tails. [d] n_{tr} = total ring number. [e] n_r = aromatic ring number.

parameters for these models are also included in Table 2. Additionally, in Table 3 are collected molecular structure features such as aliphatic tail number, n_t, total carbon number at the tails, n_c, total ring numbers, n_{tr}, aromatic ring number, n_r, heteroatom numbers, and the n_r/n_c ratio describing each asphaltene molecule. From simple examination of Tables 2 and 3, it is clear that molecules with large n_c and small n_r exhibit the biggest value of δ while molecules with small n_c and large n_r show the smallest δ values. As well, it can be seen that, the n_r/n_c ratio roughly follows the same tendency of δ. In fact, a good cubic correlation (see Figure 3) between both parameters has been found: $\delta = 5.967(n_r/n_c) - 3.062(n_r/n_c)^2 + 0.507\ (n_r/n_c)^3 + 16.593$ with $R^2 = 0.965$.

To perform a rigorous structure−solubility parameter relationship study, we have chosen several molecular connectivity indices that encode specific attributes of structures and provide a formal mathematical characterization of molecules,[19] and a genetic function approximation (GFA) algorithm[20] was used to build the functional models. The first step is to investigate if the data is normally distributed. Most regression algorithms rely on the investigated data being normally distributed. A univariate analysis and a simple solubility parameter plot have shown that Mu3, RH3, and RH4 models are outside the normal distribution. Therefore, those models were eradicated from the data. At the second step, φ and χ connectivity indices were calculated. Table 4 shows the obtained values of those indices for the studied asphaltene molecules. We can see that in effect φ counts the number of atoms with sp^3 hybridization on the carbon chains given flexibility to the molecules: its value systematically decreases from the R1 model (23.797) to the M1 (2.466) model, which contain the maxima and minima numbers of aliphatic chains, respectively. Inspection of Tables 3 (column 4) and

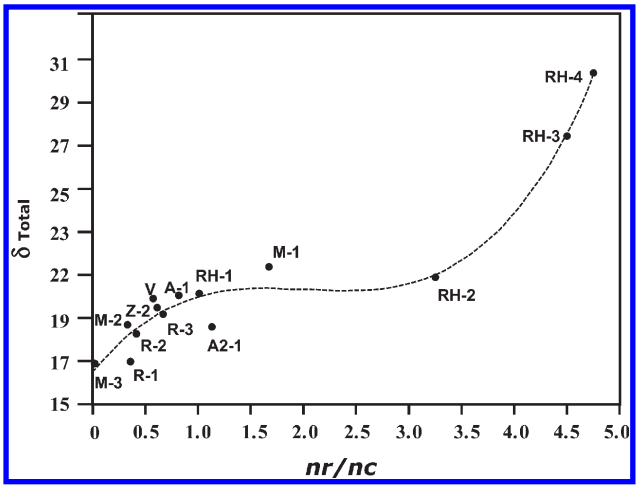

Figure 3. Total solubility parameters of the asphaltene models as a function of the n_r/n_c ratio.

4 (column 4) shows that φ is related to n_c (the total number of carbon atoms at the tails). A linear correlation $\varphi = 0.317n_c + 3.550$ with $R^2 = 0.98$ confirms the information encoded by the flexibility index. In the same way, comparing the values of χ with the structure features collected in Table 3, we can see that each of those χ indices is related to n_{tr} and n_t, the total number of rings (aromatic or not) and aliphatic chains, respectively. For example, $^3\chi_c$ for RH2, RH3, and RH4 ($n_{tr} = 19$ and $n_t = 4$) exhibit just the same value of 5.819, while A1 and RH1 ($n_{tr} = 19$ and $n_t = 5$) show an increased same value of 6.230. R3 ($n_{tr} = 25$ and $n_t = 7$) and R1 ($n_{tr} = 26$ and $n_t = 11$) enclose values of 9.245 and 12.380, respectively. All of the χ indices show exactly the same trend with respect to n_{tr} and n_t.

At the next step a correlation matrix was generated. A correlation matrix is a table of all possible pairwise correlation coefficients for a set of variables. It was found that the indices that most highly correlated with the solubility parameters include φ and $^1\chi$. Additionally we have also found that all of the χ indices are highly correlated. Finally, the GFA was performed and the following relationship $\delta = -0.361561\varphi + 0.000698(^1\chi)^2 + 22.187554$ with $R^2 = 0.925$ and cross-validated $R^2 = 0.851$ was obtained. The accuracy of this model is not good enough, as indicated by the difference between R^2 and cross-validated R^2 values. Appreciable residual (the difference between the predicted value and the actual value) close to 0.64 for R2 and VI was obtained. Nevertheless, the above relationship let us interpret the solubility parameter directly in terms of significant aspects of molecular structure. Thus, the φ index contributes with 60% of the predicted δ and with a negative coefficient; the model indicates that the solubility parameter generally decreases with the flexibility (and branching) provided by the aliphatic chains. Inclusion of more χ indices usually improves the fitting of the models; however, we have to keep in mind the strong correlation observed between all of the χ indices. For example, a really good accuracy, practically without residual, is provided by the following models: $\delta = -0.31141(^1\chi) + 0.55827(^3\chi) - 2.57557(^3\chi_c) - 0.01127(\varphi)^2 + 0.12973(^3\chi_c)^2 + 23.27960$ with $R^2 = 0.999$ and cross-validated $R^2 = 0.994$. Unfortunately, we cannot see information in those formal connectivity indices about the role of aromatic ring forming the fused aromatic ring core such as that provided by our empirical n_r/n_c parameter.

A final commentary in this section is about the H/C ratio. This ratio is an important parameter which measures aromaticity: In general, the

Table 4. Values of Structural and Kier−Hall Topological Descriptors for the Asphaltenes Molecules

asphaltene	δ	φ	$^0\chi$	$^1\chi$	$^2\chi$	$^3\chi_p$	$^3\chi_c$
R1	16.997	23.797 20	101.656 59	71.600 80	70.104 49	61.621 97	12.380 41
R2	18.292	11.187 15	47.144 46	33.700 99	31.380 40	29.259 12	4.858 318
M2	18.705	10.753 77	35.768 66	25.537 08	22.523 41	19.850 88	2.891 084
R3	19.182	15.901 62	79.657 37	57.568 33	55.621 80	52.647 69	9.244 93
ZJ	19.480	9.238 90	39.354 08	29.101 71	26.826 04	24.642 54	3.568 709
VI	19.908	9.506 78	36.760 22	26.617 74	23.356 05	21.551 58	2.745 728
A1	20.045	8.709 36	51.625 08	38.143 41	37.655 22	36.661 15	6.230 285
RH1	20.152	7.779 74	49.503 76	36.643 41	36.594 56	35.911 15	6.230 285
RH2	20.872	5.456 29	42.813 52	32.300 88	33.115 99	33.272 84	5.818 196
M1	21.353	2.466 43	15.551 68	11.258 35	10.502 43	9.678 599	1.592 686

Table 5. Relative Solubility of Asphaltene Models in Toluene and *n*-Heptane

models	ΔS_R in Tol	RED in Tol	RED1 in Tol	ΔS_R in Hep	RED in Hep
M3	0.389	0.833	1.342	0.448	0.629
R1	0.145	0.615	0.990	0.117	0.866
A2_2	0.763	0.338	0.544	0.126	1.014
R2	0.969	0.535	0.862	0.046	1.183
A2_1	0.999	0.010	0.016	0.022	1.352
		0.760 [a]	0.760		1.440
M2	0.996	0.312	0.503	0.042	1.354
R3	0.827	0.320	0.518	0.000	1.538
ZJ	0.762	1.052	1.694	0.005	1.668
VI	0.647	0.564	0.908	0.005	1.806
A1	0.476	0.788	1.270	0.000	1.862
		1.270 [a]	1.270		2.110
RH1	0.196	0.824	1.328	0.000	1.904
RH2	0.215	1.064	1.714	0.000	2.180
M1	0.451	1.288	2.074	0.022	2.374
RH3	0.000	2.859	4.606	0.000	4.071
RH4	0.000	3.625	5.839	0.000	4.798

[a] Reference 18

molecule aromaticity increases as H/C ratio decreases. H/C ratio was experimentally determined[26,27] for asphaltenes isolated from Ceuta (API = 29−32), Furrial (API = 21.0), DM-153 (API = 14.0), Boscan (API = 10.3), and Cerro Negro (API = 8.5) crude oils. Values of 0.97, 0.97, 1.21, 1.21, and 1.12−1.17 were obtained, respectively. For A1 and A2 fraction from Furrial crude, values of 0.92 and 1.020 were obtained, respectively. The H/C calculated values at this work (column 3 of Table2) show that the M3 model without aromatic rings and RH2, M1, RH3, and RH4 models with full aromatic rings are outside of the experimental range: 0.90−1.21. The remainder models exhibit typical H/C ratio values of asphaltene molecules. This result supports the eradication of these models from the data in order to obtain a normal distribution.

4. 2. Asphaltenes Solubility in Toluene and Heptane. In the present work, the calculated ΔS_R and RED values for the studied asphaltene models in toluene and heptane are reported in Table 5. The ΔS_R values suggest that A2_2, R2, A2_1, M2, R3, ZJ, and VI models should be soluble in toluene while A1, RH1, RH2, M1, RH3, RH4, M3, and R1 models should not be. All of the models are predicted to be insoluble in heptane. The obtained trend for solubility (maxima solubility corresponds to $\Delta S_R = 1$) in toluene is

$$A2_1 \approx M2 \approx R2 > R3 > A2_2 = ZJ > VI > A1 \approx M1 > M3 > RH2 > RH1 \approx R1 > RH3 = RH4$$

To calculate the RED parameter using eq 3 is essential to knowing R_0 for each asphaltene molecule. R_0 is very important for fixing the borderline between good solvents (RED < 1) and bad solvents (RED > 1). By definition R_0 is an experimental parameter and has to correspond to the radius of a sphere centered at each asphaltene molecule containing inside the maximum number of good solvents and bad solvents outliers. Values[21] of R_0 equal to 5 $MPa^{0.5}$ for solutions of asphaltenes in organic liquids and 5.3 for asphaltenes obtained from Venezuelan bitumen[17b] have been reported. This last value of R_0 was used to calculate the RED values reported in Table 5. The trend of solubility (maxima solubility corresponds to RED = 0) in toluene suggested by RED is

$$A2_1 >> A2_2 \approx R3 \approx M2 > R2 \approx VI \approx R1 > A1 > M3 > ZJ \approx RH2 > M1 > RH3 > RH4$$

It is quite different from the ΔS_R suggestion. Note that this last parameter suggests a very low solubility ($\Delta S_R = 0.145$) of R1 in toluene, while RED predicts an appreciable solubility. According to ΔS_R A2_1 ($\Delta S_R = 0.999$), M2 ($\Delta S_R = 0.996$), and R2 ($\Delta S_R = 0.969$) should present very similar solubility while RED suggests that A2_1 is by far more soluble than the other asphaltenes. Recently,[18] experimental values of RED in toluene for asphaltene, A1, and A2 fractions isolated from Hamaca crude were reported to be 0.72, 1.27, and 0.76, respectively. The corresponding calculated values (see Table 5) are very different of these experimental values. Therefore we have fitted R_0 to obtain exactly the same RED value of A1 asphaltene, and the results are shown in column 4 (called RED1). As is expected, the predicted solubility trend by RE1 is exactly the same as that predicted by the previous RED. However, now M3, ZJ, A1, RH1, RH2, M1, RH3, and RH4 models are predicted to be insoluble in toluene. R1, R2, and VI are borderline while A2_2, M2, R3, and specially A2_1 are predicted to be miscible in toluene.

Additionally, from inspection of Tables 5 and 3 it can be seen that the M3 and R1 models with a large number and length of aliphatic tails (n_C = 25 and 66 for M3 and R1, respectively) should have small relative solubility in toluene ($RED_{M3} = 1.342$, $RED_{R1} = 0.990$) and at the same time the biggest one in

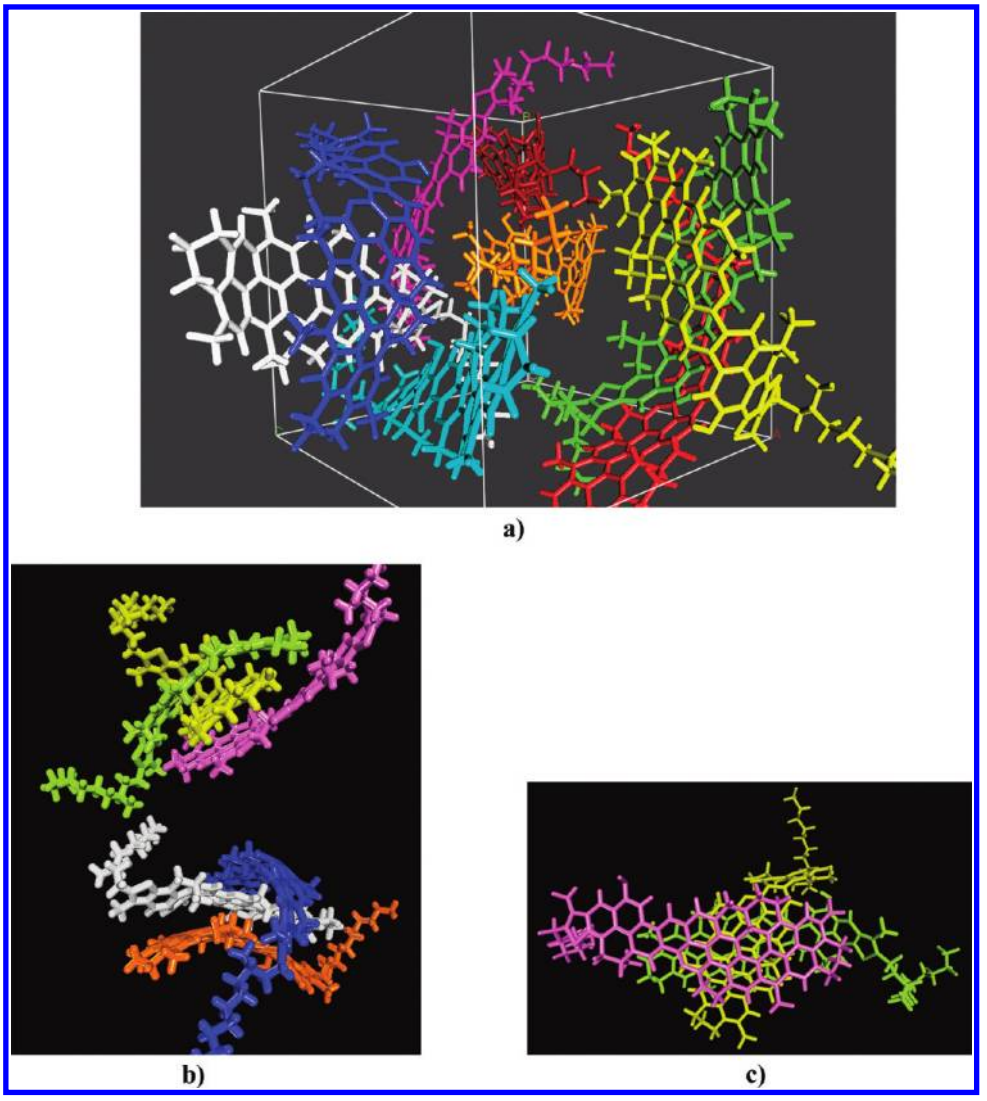

Figure 4. (a) Simulation box (unit cell of the periodic system) containing 10 A1 molecules showing a snapshot at a point of the dynamic trajectory. The bulk of the asphaltene is obtained by means of periodic repetition of the unit cell. (b) Side and (c) top view of typical asphaltene bulk aggregates (trimers) showing the stacking of aromatic ring core systems.

Table 6. Resins Density, Molar Volume, and Solubility Parameter in Toluene and *n*-Heptane Estimated from *NPT* Molecular Dynamic Simulations

models	ρ (g/cm^3)	V_m (cm^3/mol)	δ (MPa$^{1/2}$)	δ_{elec} (MPa$^{1/2}$)	δ_{vdW} (MPa$^{1/2}$)
Noram C	0.783	236.542	17.391	3.994	16.924
Athabasca	0.963	332.700	17.768	3.197	17.475
OL1 native	0.949	716.842	18.014	5.849	17.034
NDP	0.906	279.550	18.816	5.102	18.108
NP	0.909	242.296	19.597	8.621	17.588
HP	0.941	189.450	20.366	10.336	17.528
SBP	1.010	148.681	21.023	11.846	17.352
6MDBT	1.199	165.321	21.618	4.686	21.094
NPE6	1.030	470.241	21.016	8.933	19.019
phenol	1.069	87.940	25.066	16.469	18.874

n-heptane (RED_{M3} = 0.629, RED_{R1} = 0.866). A check up of Table 3 confirms that, in general, the increase of aliphatic chain number can dramatically increase the asphaltene solubility in aliphatic solvents such as heptane but a decrease in toluene. This trend is balanced by the aromatic rings presence: the increase of aromatic rings number produces a systematic solubility decrease of asphaltenes in toluene and heptane. Note that (in Table 4) the diminution of the length of the aliphatic chain from -C_{12} in A1 to -C_1

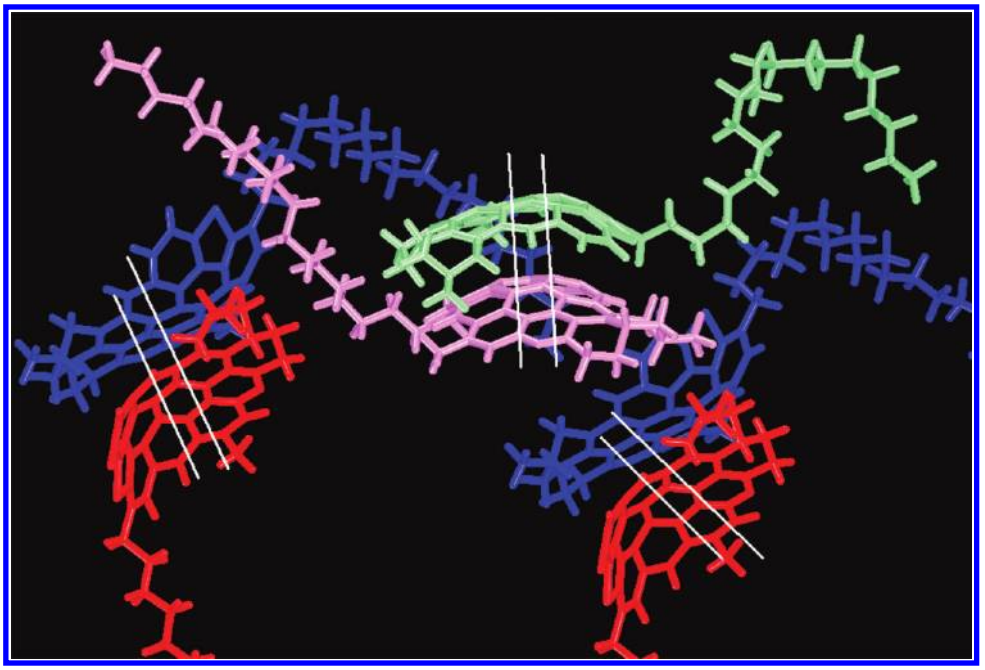

Figure 5. Snapshot of ZJ asphaltene models at a point of the dynamic trajectory showing the typical stacking of the core of aromatic rings. Parallel white lines highlight the core−core interactions. Mainly as a consequence of the temperature and vibrational movement, the molecules at a typical trajectory point could show bending or distortion with respect to the geometry of minimum energy. We have observed appreciable bending for molecules with large aliphatic tails and an elongated aromatic fused core.

in RH2 produces a change of RED1 from 1.270 to 1.328 in toluene. Additional modification of four aliphatic rings in the core of A1 to four aromatic rings in RH3 drastically increases RED1 to 4.606 in toluene. In Tables 5 and 3, we can also see that the R3 model with a really big aromatic core (23 rings), but seven -C_5 chains shows a value of RED1 equal to 0.518, suggesting miscibility in toluene. However, increasing the number and length of the aliphatic chains to 11 and C_7, respectively, as in the R1 model, RED1 drastically increases to 0.990, suggesting a low solubility in toluene. These results clearly suggest that, in order to obtain miscibility of asphaltene molecules in toluene, a balance between the number of aromatic rings at the core and the number and length of the aliphatic chains have to exist. On the contrary, in heptane the M3 model without aromatic rings shows the most appreciable solubility (RED = 0.629).

Inspection of Table 2 shows that the dispersive component, δ_{vdW}, systematically increase from M3 (no aromatic rings) to RH4 (full aromatic rings). ZJ, VI, A1, RH1, RH2, M1, RH3, and RH4 showing the smallest solubility in toluene have a δ_{vdW} value bigger than 19.0 $MPa^{0.5}$ while the biggest solubility is showed by models with 17.0 < δ_{vdW} < 18.7 $MPa^{0.5}$. These findings agree with previous conclusions reported in ref 4, suggesting that molecular interactions in asphaltenes are dominated by van der Waals binding via stacking of aromatic rings vs steric repulsion associated with alkane chains. Figures 4−6 show snapshots of the molecular configurations at chosen points of the dynamic trajectories for A1, ZJ, and M1 models, respectively. Typical trimers formed in A1 can be observed. We can see that, for each aggregate, the ring cores are stacked via $\pi-\pi$ interactions and the large aliphatic tails are farthest away. A similar configuration for the produced aggregates in ZJ (Figure 5) was also observed. In this case a lot of dimers such as the aggregates shown in Figure 4 are created. Figure 6 shows that, for the M1 model, containing a really small aliphatic chain (-CH_3), practically all of the molecules are participating in $\pi-\pi$ interactions. Thus, the observed aggregates pattern confirms the role of the aromatic core stacking in the interactions of the molecule asphaltenes.

4. 3. Asphaltene Solubility in Amphiphiles. Asphaltenes precipitation depends on the colloidal stability of crude oils. Asphaltenes and resins compose the disperse phase of this colloidal system, forming small nanoaggregates while maltenes are the continuous phase.[34] There is no doubt regarding the important role played by resins in the behavior of asphaltenes: resins help asphaltenes to stay in solution. The activity of resins as asphaltenes stabilizers is directly related to the adsorption of the resins on the asphaltenes surfaces.[34] Several experimental and theoretical studies to explore the effect of the resins chemical structure on asphaltenes stabilization have been done.[34−42] Spectroscopic (UV, FTIR, SAXS, and fluorescence), thermodynamic (calorimetric titrations, thermogravimetric analysis, and adsorption isotherms), and other experimental methodologies involving dielectric constants or refractive index have been used to explore the effect of the nature of the resins headgroup and R alkyl chains on the effectiveness of asphaltene solubilization. In general, it has been concluded that this effectiveness is primarily controlled by the polarity of the resiṅs headgroup and the length and degree of branching of R: head with high acidity and chains with at least six C atoms were found to be required. Theoretical calculations using *NVT* molecular dynamic simulations[30,34] have found that the activity of the amphiphiles as asphaltene stabilizer increases as their adsorption on the asphaltene is more favorable. Additionally, this same study has also found that a particular balance between the polarizability and the dipole moment of the amphiphiles is needed to obtain a maximum in the adsorption energy of the amphiphiles on the asphaltenes. From a very different theoretical approach, using the solubility parameters calculated by means of the group contribution method of Van Krevelen and inside the framework of the Hansen sphere

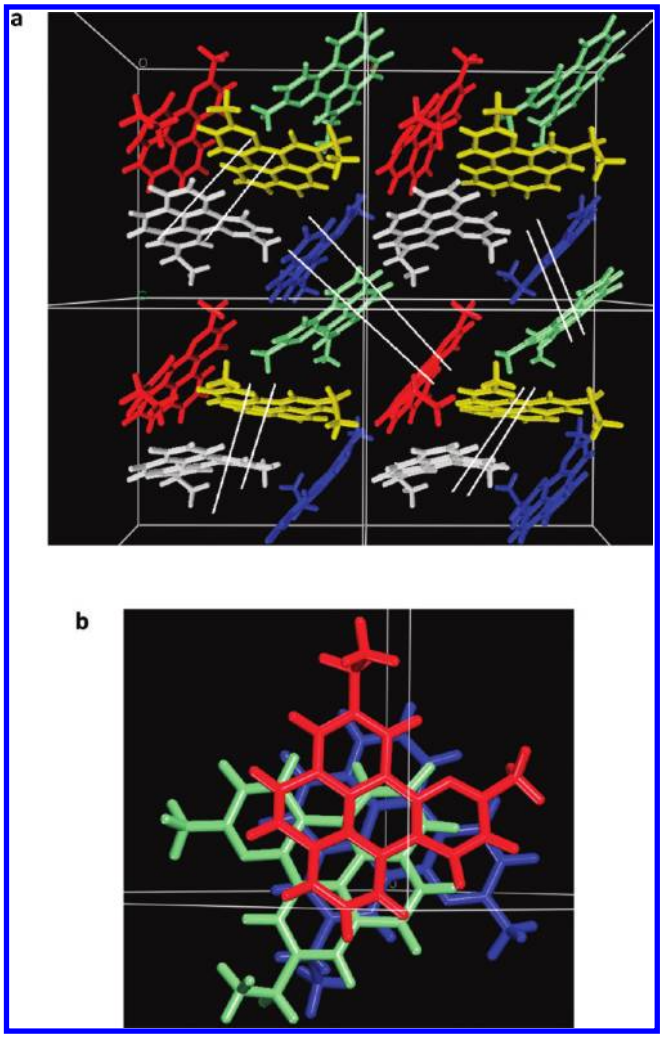

Figure 6. (a) Simulation box containing M1 molecules showing a snapshot at a point of the dynamic trajectory. Parallel white lines highlight the core−core interactions. (b) Top view of asphaltene aggregates showing the typical stacking of aromatic ring core systems.

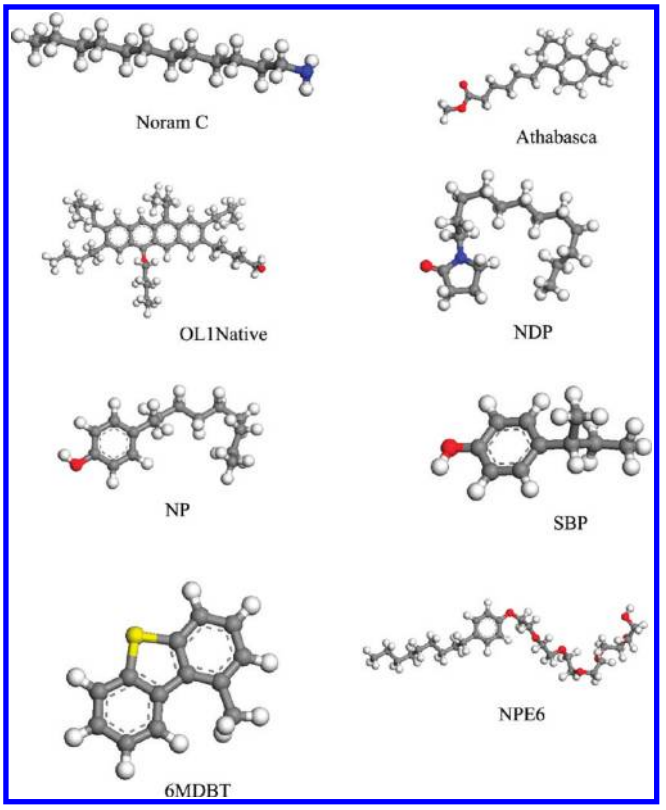

Figure 7. Ball and sticks models of the amphiphile molecules used in this work. Gray, white, red, blue, and yellow spheres denote the carbon, hydrogen, oxygen, nitrogen, and sulfur atoms, respectively.

methodology, the asphaltene−resin interactions were studied.[21] The obtained results suggested that a stabilizing effect can be expected if the dispersion part of δ of the resin corresponds to that of asphaltenes and the hydrogen bonding plus the electrostatic parts is less than 10.4 MPA. Recently, using a similar RED method a high affinity between Hamaca asphaltenes and native resins was found,[18] which is consistent with the well-known affinity of asphaltenes by resins.[43,44] Values of 0.37, 0.41, and 0.90 were reported for resins in Hamaca asphaltenes, A2, and A1 fraction, respectively.[18] Thus, asphaltenes and A2 should be dissolved rather than dispersed by resins, and compared to A2, fraction A1 is less soluble in resins.

To explore those findings, we have carried out *NPT* simulations for the following set of amphiphiles (see Figure 7): pyrrolidone (NDP),[30] *p*-(*n*-nonyl)phenol (NP), *p*-hexylphenol (HP), *p*-(*sec*-butyl)phenol (SBP),[30,21,35,36,45] *p*-(nonyl)phenol ethoxylated (NPE6),[29] Noram C,[45] Athabasca, 6-methyl DBT (6MDBT),[46] and the OL1 native resin.[47] The density (g/cm^3), molar volume (cm^3), and solubility parameter (MPa$^{0.5}$) values resulting from the *NPT* simulations are collected in Table 6 while in Table 7 are collected the characteristic aliphatic tails number, total carbon number at the tail, n_c, aromatic ring number, n_r, heteroatom numbers, and the n_r/n_c ratio describing each amphiphile molecule. It can be seen that, in general, the resins solubility parameters follow the same behavior of the asphaltene molecules. Phenols, with just one aromatic ring and one -OH group and without aliphatic chains show the biggest δ value. Increasing the length of an aliphatic chain at the -p position in SBP, HP, and NP from C_4 to C_9 systematically produces an appreciable decrease in δ from 25.066 at phenol to 19.597 MPa$^{0.5}$ at NP. Table 6 data show that the origin of this δ decreasing is mainly the noticeable diminution of the δ_{elec} component of these molecules from 16.469 MPa$^{0.5}$ in phenol to 8.621 MPa$^{0.5}$ in NP. Note that phenolic amphiphiles exhibit the largest δ_{elec} values of the studied set. Noram C and Athabasca with no aromatic rings and large aliphatic chains exhibit the smallest δ value. The OL1 native model with the largest number of aromatic rings however surrounded by six -C_5 chains shows a δ value as low as those of the Athabasca and NDP resins. Thus, OL1 native shows a behavior similar to that observed by the R1 asphaltene model.

Using the δ values of Tables 2 and 6, we have calculated the RED for the studied amphiphiles in A2_1, R3, A1, RH2, M1, and RH3 using the experimental R_0 for A1 and A2 fractions isolated from a Venezuelan crude (Hamaca crude from the Orinoco's belt).[18] These asphaltene models were chosen in order to emphasize the effect of increasing the aromatic ring numbers and decreasing the length and numbers of the aliphatic chains. The obtained results are collected in Table 8. It can be seen that A2_1, the archipelago model, and RH3, the almost completely continental model, exhibit opposite behavior. A2_1 is soluble in almost the entire range of amphiphiles, except in phenol, while

Table 7. Structural Characteristics of the Amphiphile Molecules

model	n_t	n_c	n_r	n_r/n_c
Noram C	1 (12)	12	0	0
Athabasca	1 (8)	8	0	0
OL1 native	6 (5)	30	4	0.133
NDP	1 (12)	12	0	0
NP	1 (9)	9	1	0.111
HP	1 (6)	6	1	0.167
SBP	1 (4)	4	1	0.250
6MDBT	1 (1)	1	3	3.000
NPE6	1 (9)	9	1	0.111
Phenol	0	0	1	

RH3 is only soluble in phenol. Extremely high δ electrostatic components are exhibited for RH3 (18.382 $MPa^{0.5}$) and phenol (16.469 $MPa^{0.5}$), showing the origin of the affinity between both molecules. In general, there is a large affinity between A2_1 and the amphiphiles containing large aliphatic tails and no aromatic rings such as NDP, Noram C, Athabasca, or aromatic rings surrounded by many aliphatic chains such as the OL1 native model. A2_1 is by far more soluble in NDP than the other amphiphiles. Comparison of the electrostatic and dispersive components of the solubility parameter (Table 4) with the respective components of A2_1 (Table 2) shows that both components are quite similar for NDP (5.102, 18.108) and A2_1 (4.965, 17.918), explaining the very low value of RED. A small decrease (around 1 $MPa^{0.5}$ unit) of the dispersive or the electrostatic component produces the decrease in the A2_1 affinity on OL1 NativE, Athabasca, and Noram C amphiphiles, while a large increase of δ_{elec} in HP (10.336) and SBP (11.846) or δ_{vdW} in 6MDBT (21.094) produces an appreciable increase of RED of those amphiphiles. Phenolic heads, containing an -OH group, generate a big electrostatic contribution which is balanced by large aliphatic chains.

Similar to the experimental finding,[18] A1 is always less soluble than A2_1 for the entire set of amphiphiles. REDs for native resins of Hamaca crude were found to be[18] 0.41 and 0.90 in A2_1 and A1, respectively. Examination of Table 8 shows that the calculated RED values for NP, 0.476 (A2) and 0.868 (A1), coincide with the experimental ones. Thus, NP shows the more similar affinity of the Hamaca native resins for A1 and A2. In general, affinity between amphiphiles and asphaltenes decreases systematically from A2_1 to RH3. An observed systematic increase of δ_{vdW} from A1 to RH3 (see Table1) can explain this methodical decrease.

For each amphiphile good polynomial regressions between RED and the characteristic n_r/n_c ratio of the asphaltenes (Table 3) have been found. For example, for Noram C, RED = $1.644(n_r/n_c) - 0.577(n_r/n_c)^2 + 0.062(n_r/n_c)^3 - 0.481$ with R^2 = 0.905. In this correlation, the value for A2_1, just the archipelago model, shows the major deviation. Removal of A2_1 produces the excellent correlation RED = $1.776(n_r/n_c) - 0.638(n_r/n_c)^2 + 0.068(n_r/n_c)^3 - 0.427$ with R^2 = 0.998 fixing all the points. Similarly an outstanding correlation for RED and δ_{vdW} was obtained: $\delta_{vdW} = 2.613(RED) + 2.814(RED)^2 - 1.614(RED)^3 + 17.012$ with R^2 = 0.999. In this correlation only the corresponding values for RH3, just the model with a really big δ_{elec} value (18.382), shows a deviation from the lineal relationship. Removal of RH3 leads to the following lineal correlation:

Table 8. RED Values of Chosen Asphaltenes in the Studied Amphiphiles

models	A2 (0.41)[a]	R3	A1 (0.90)[a]	RH2	M1	RH3
Noram C	0.284	0.453	0.728	0.925	1.064	2.042
Athabasca	0.253	0.343	0.584	0.786	0.922	2.081
OL1 Native	0.254	0.463	0.764	0.934	1.078	1.817
NDP	0.052	0.175	0.474	0.644	0.787	1.796
NP	0.476	0.614	0.868	0.977	1.109	1.437
HP	0.696	0.828	1.055	1.140	1.264	1.258
SBP	0.894	1.019	1.244	1.317	1.435	1.135
6MDBT	0.815	0.621	0.381	0.187	0.155	1.767
NPE6	0.583	0.593	0.732	0.766	0.875	1.258
Phenol	1.495	1.554	1.689	1.682	1.758	0.449

[a] Reference 18.

RED = $0.249(\delta_{vdW}) - 4.193$ with R^2 = 0.999. Similar correlations were found for each studied amphiphiles. An exception takes place for 6MDBT that is opposite to the other amphiphiles; its affinity for the asphaltenes substantially increases from A2_1 to M1. The following correlations RED = $-0.217(\delta_{vdW}) + 4.691R^2$ = 0.987 and RED = $-0.342(n_r/n_c) - 0.091(n_r/n_c)^2 + 0.029(n_r/n_c)^3 + 0.816R^2$ = 0.993 were determined. Note that 6MDBT exhibits the largest dispersive component (21.094) of the studied amphiphiles. Contrary to A2_1, the molecules of A1, RH2, and M1 show high affinity for amphiphiles containing aromatic rings and small aliphatic chains such as 6MDBT. In general, these results agree and confirm the reference[21] finding that suggested that amphiphiles stabilizing effect can be expected if δ_{vdW} is similar to the asphaltene and δ_{elec} < 10.4 $MPa^{0.5}$. We have found that the best amphiphiles for the studied set of asphaltenes (except RH3) show δ_{elec} < 5.9. In summary, archipelago model A2_1 shows a large affinity by amphiphiles containing large aliphatic tails and no aromatic rings or aromatic rings surrounded by many aliphatic chains. A2_1 is by far more soluble on those kinds of amphiphiles than the continental models, and as a consequence of a systematic increase of asphaltenes δ_{vdW}, affinity between those amphiphiles and asphaltenes decreases systematically from A2_1 to RH3. These continental models exhibit large affinity for amphiphiles containing a core of aromatic rings and small aliphatic chains.

These results agree the Acevedo et al.[18] suggestion about the structure of a Hamaca oil asphaltene particle. Since affinity of an amphiphile such as nonyl−phenol for the asphaltenes archipelago (A2) and continental fraction (A1) is very high (RED = 0.476) and very low (RED = 0.868), respectively, A1 should occupy the particle core while A2 should be in the periphery and in close contact with the nonyl−phenol molecules.

5. CONCLUSIONS

The solubility parameters, δ, of a set of asphaltenes and amphiphiles were calculated using a molecular dynamic atomistic *NPT* ensemble. The following relationship between δ and the molecular structure was found: the increase of the number of aromatic rings forming the asphaltenes core and the decrease of the number (and length) of aliphatic chains attached to that core produce the increase of δ. Molecules with large total carbon atom number at the tails, n_c, and small aromatic ring number, n_r, exhibit the biggest values of δ, while molecules with small n_c and large n_r show the smallest δ values. A good polynomial correlation $\delta = 5.967(n_r/n_c) - 3.062(n_r/n_c)^2 + 0.507(n_r/n_c)^3 + 16.593$ with R^2 = 0.965 supports this finding.

The solubility of the asphaltenes in toluene and heptane was explored using the calculated δ and the sphere method of Hansen. The results confirm that the increase of n_r produces a systematical solubility decrease of asphaltenes in toluene and heptane. At the same time, the increase of n_c can dramatically increase the asphaltenes solubility in aliphatic solvents such as heptane but a decrease in toluene. It was also found that δ_{vdW} systematically increases as n_r increases, suggesting that molecular interactions in asphaltenes are dominated for van der Waals binding via stacking of aromatic rings vs steric repulsion associated with alkane chains. The core−core stacking completely dominates in continental asphaltenes containing a large aromatic core and small aliphatic tails, and consequently these kinds of asphaltenes are predisposed to form a separated phase in solvents such as toluene and heptanes.

A similar study for solubility of asphaltenes in a set of amphiphiles has shown that the archipelago asphaltenes model A2_1 is soluble in almost the entire amphiphiles, except in phenol which exhibits an extremely high δ_{elec} component. A2_1 is more soluble in the amphiphiles than the continental asphaltenes models. In general, affinity between amphiphiles and asphaltenes decreases systematically following a systematic increase of asphaltenes δ_{vdW}. Thus, an excellent linear correlation between the RED for each asphaltenes in the amphiphiles and the respective asphaltenes δ_{vdW} (for example for Noram C is RED = $0.249\delta_{vdW} - 4.193$ with $R^2 = 0.999$) was found. An exception takes place for 6MDBT that is opposite to the other amphiphiles; its affinity for the asphaltenes substantially increases as δ_{vdW} increases: RED = $-0.217(\delta_{vdW}) + 4.691R^2 = 0.987$. In general, there is a large affinity between the archipelago model A2_1 and the amphiphiles containing large aliphatic tails and no aromatic rings, while continental models show high affinity for amphiphiles containing aromatic rings and small aliphatic chains such as 6MDBT.

AUTHOR INFORMATION

Corresponding Author

*Tel.: +58-212-5041336. Fax: +58-212-5041350. E-mail: yaray@ivic.gob.ve.

6. ACKNOWLEDGMENT

The financial support provided by the Fonacyt Grant (G-2005000424) is gratefully acknowledged.

SYMBOLS USED

ΔS_R = Scatchard−Hildebrand relative solubility
RED = Hansen measurement of solubility
δ = General representation of Hansen solubility parameters
δ_{vdW} = van der Waals or dispersion component of the solubility parameter
δ_{ES} = Electrostatic component of the solubility parameter
NPT = Molecular dynamic simulation at constant composition, pressure and temperature
R1, R2, R3, M1, M2,
ZJ, VI, A1, A2_1, A2_2 = Asphaltene molecules proposed at refs,[31,30,11,29,32,33,26] and[27]
RH1, RH2, RH3, RH4 = Models created from the A1 model removing aliphatic chains and increasing the aromatic ring numbers
n_t = Aliphatic chain numbers attached to the aromatic ring core
n_C = Total carbon atoms at the aliphatic tails
n_r = Aromatic ring number at the asphaltenes core
NDP, NP, HP, SBP,
NPE6, 6MDBT = pyrrolidone, p-(n-Nonyl) phenol, p-Hexyl phenol, p-(sec-butyl)phenol, p-(Nonyl)-phenol ethoxylated, 6-methyl molecules of amphiphiles

REFERENCES

(1) Leon, O.; Contreras, E.; Rogel, E. *Colloids Surf., A* **2001**, *189*, 123–130.
(2) Pineda, L.; Trejo, F.; Ancheyta, J. *Petrol. Sci. Technol.* **2007**, *25*, 105–119.
(3) Crick, F. *Phys. Today* **2002**, *55*, 62–63.
(4) Andreatta, G.; Goncalves, C. C.; Buffin, G.; Bostrom, N.; Quintella, C. M.; Arteaga-Larios, F.; Perez, E.; Mullins, O. C. *Energy Fuels* **2005**, *19*, 1282–1289.
(5) Zhang, S.-H.; Sun, L.-L.; Xu, J.-B.; Wu, H.; Wen, H. *Energy Fuels* **2010**, *24*, 4312–4326.
(6) Merdrignac, I.; Espinat, D. *Oil Gas Sci. Technol.* **2007**, *62*, 7–32.
(7) Kharrat, A. M.; Zacharia, J.; Cherian, V. J.; Anyatonwu, A. *Energy Fuels* **2007**, *21*, 3618–3621.
(8) Zhang, L.; Greenfield, M. L. *Energy Fuels* **2007**, *21*, 1712–1716.
(9) Murgich, J.; Rodríguez, J.; Aray, Y. *Energy Fuels* **1996**, *10*, 68–76.
(10) Artok, L.; Su, Y.; Hirose, Y.; Hosokawa, M.; Murata, S.; Nombra, M. *Energy Fuels* **1999**, *13*, 287–296.
(11) Groenzin, H.; Mullins, O. C. *Energy Fuels* **2000**, *14*, 677–684.
(12) Rogel, E.; Carbognani, L. *Energy Fuels* **2003**, *17*, 378–386.
(13) Takanohashi, T.; Sato, S.; Saito, I.; Tanaka, R. *Energy Fuels* **2003**, *17*, 135–139.
(14) Gray, M. R. *Energy Fuels* **2003**, *17*, 1566–1569.
(15) Sheremata, J. M.; Gray, M. R.; Dettman, H. D.; McCaffrey, W. *Energy Fuels* **2004**, *18*, 1377–1384.
(16) Siskin, M.; Kelemen, S. R.; Eppig, C. P.; Brown, L. D.; Afeworki, M. *Energy Fuels* **2006**, *20*, 1227–1234.
(17) (a) Hansen, C. M.; *Hansen Solubility Parameters: A User's Handbook*; CRC Press: Boca Raton, FL, 1999; ISBN:0-8493-1525-5. (b) Redelius, P. *Energy Fuels* **2004**, *18*, 1087–1092.
(18) Acevedo, S.; Castro, A.; Vásquez, E.; Marcano, F.; Ranaudo, M. A. *Energy Fuels* **2010**, *24*, 5921–5933.
(19) Hall, L. H.; Kier, L. B. *J. Mol. Graph. Modell.* **2001**, *20*, 4–18.
(20) (a) Roberto, T.; Viviana, C. *Molecular Descriptors for Chemoinformatics*; Wiley, VCH Verlag: Weinheim, Germany, 2009. (b) Khaled, K. F.; *Corros. Sci.*, in press (doi: 10.1016/j.corsci.2011.01.035).
(21) Laux, H.; Rahimian, I.; Butz, T. *Fuel Process. Technol.* **2000**, *67*, 79–89.
(22) (a) Belmares, M.; Blanco, M.; Goddard, W. A., III; Ross, R. B.; Caldwell, G.; Chou, S. H.; Pham, J.; Olofson, P. M.; Thomas, C. *J. Comput. Chem.* **2004**, *25*, 1814–1826. (b) Diallo, M. S.; Strachan, A.; Faulon, J.; Goddard, W. A., III *Pet. Sci. Technol.* **2004**, *22*, 877–899.
(23) *Discover* (available as part of Material Studio); Accelrys: San Diego, CA, USA, 2010.
(24) (a) *DMol*^{3} (available as part of Material Studio); Accelrys: San Diego, CA, USA, 2010. (b) Delley, B. *J. Chem. Phys.* **1990**, *92*, 508–517. (c) **2000**, *113*, 7756–7764.
(25) (a) Sun, H. *J. Phys. Chem. B* **1998**, *102*, 7338–7364. (b) Eichinger, B. E.; Rigby, D.; Stein, J. *Polymer* **2002**, *43*, 599–607. (c) Eichinger, B. E.; Rigby, D.; Muir, M. H. *Comp. Polym. Sci.* **1995**, *5*, 147–163. (d) Gupta, J.; Nunes, C.; Vyas, S.; Jonnalagadda *J. Phys. Chem. B* **2011**, *115*, 2014–2023. (e) Rogel, E. *Energy Fuels* **2011**, *25*, 472–481. (f) Barton, A. F. M. *Chem. Rev.* **1975**, *75*, 731–753. (g) Derecskei, B.; Derecskei-Kovacs, A. *Mol. Simul.* **2008**, *34*, 1167–1175.
(26) (a) Acevedo, S.; Escobar, O.; Echevarria, L.; Gutiérrez, L. B.; Méndez, B. *Energy Fuels* **2004**, *18*, 305–311. (b) Acevedo, S.; Gutiérrez, L. B.; Negrin, G.; Pereira, J. C.; Méndez, B.; Delolme, F.; Dessalces, G.; Broseta, D. *Energy Fuels* **2005**, *19*, 1548–1560.

(27) Acevedo, S.; Castro, A.; Negrin, J. G.; Fernández, A.; Escobar, G.; Piscitelli, V. *Energy Fuels* **2007**, *21*, 2165–2175.
(28) (a) Groenzin, H.; Mullins, O. C. *J. Phys. Chem. A* **1999**, *103*, 11237–11245. (b) Mullins, O. C.; Betancourt, S. S.; Cribbs, M. E.; Dubost, F. X.; Creek, J. L.; Ballard Andrews, A.; Venkataramanan, L. *Energy Fuels* **2007**, *21*, 2875–2882.
(29) Groenzin, H; Mullins, O. C. *Petrol. Sci. Technol.* **2001**, *19*, 219–230.
(30) Rogel, E.; Contreras, E.; y León, O. *Petrol. Sci. and Technol.* **2002**, *20*, 725–739.
(31) Rogel, E. *Colloids Surf., A* **1995**, *104*, 85–93.
(32) Zajac, G. W.; Sethi, N. K.; Joseph, J. T. *Scanning Microsc.* **1994**, *8*, 463–470.
(33) Kuznicki, T.; Masliyah, J. H.; Bhattacharjee, S. *Energy Fuels* **2009**, *23*, 5027–5035.
(34) Rogel, E. *Energy Fuels* **2008**, *22*, 3922–3929.
(35) Hernandez-Trujillo, J.; Martinez-Magadán, J. M.; Garcia-Cruz., I. *Energy Fuels* **2007**, *21*, 1127–1132.
(36) Chang, C. L.; Fogler, H. S. *Langmuir* **1994**, *10*, 1749–1757.
(37) Koots, J. A.; Speight, J. G. *Fuel* **1975**, *54*, 179–184.
(38) Wiehe, I. A.; Jermansen, T. G. *Pet. Sci. Technol.* **2003**, *21*, 527–536.
(39) Leon, O.; Rogel, E.; Urbina, A.; Andújar, A.; Lucas, A. *Langmuir* **1999**, *15*, 7653–7657.
(40) Merino-Garcia, D.; Andersen, S. I. *Langmuir* **2004**, *20*, 1473–1480.
(41) Merino-Garcia, D.; Andersen, S. I. *Pet. Sci. Technol.* **2003**, *21*, 507–525.
(42) Hu, Y. F.; Guo, T. M. *Langmuir* **2005**, *21*, 8168–8174.
(43) Acevedo, S.; Rodriguez, P.; Zuloaga, C. *Energy Fuels* **2008**, *22*, 2332–2340.
(44) Leon, O.; Contreras, E.; Rogel, E.; Dambakli, G.; Acevedo, S. *Langmuir* **2002**, *18*, 5106–5112.
(45) González, G.; Middea, A. *Colloids Surf.* **1991**, *52*, 207–217.
(46) Aguilera-Mercado, B.; Herdes, C.; Murgich, J.; Muller, E. A. *Energy Fuels* **2006**, *20*, 327–338.
(47) Leon, O.; Contreras, E.; Rogel, E.; Dambakli, G.; Espidel, J.; Acevedo, S. *Energy Fuels* **2001**, *15*, 1028–1032.